

# Dynamics of water at the interface of a small protein, enterotoxin

Sundaram Balasubramanian\*, Sanjoy Bandyopadhyay<sup>†</sup>, Subrata Pal<sup>‡</sup> and Biman Bagchi<sup>‡,\*</sup>

Chemistry and Physics of Materials Unit, Jawaharlal Nehru Centre for Advanced Scientific Research, Jakkur, Bangalore 560 064, India

<sup>†</sup>Department of Chemistry, Indian Institute of Technology Kharagpur, Kharagpur 721 302, India

<sup>‡</sup>Solid State and Structural Chemistry Unit, Indian Institute of Science, Bangalore 560 012, India

**Fully atomistic molecular dynamics simulations have been carried out to investigate the correlation of biological activity with dynamics of water molecules in an aqueous protein solution of the toxic domain of enterotoxin (PDB ID: 1ETN). This is a small protein of 13 amino acid residues. Our study of this water soluble protein clearly reveals that water dynamics slows down in the hydration layer. Despite this general slowing down, water molecules in the vicinity of the second  $\beta$  turn of this protein exhibit faster dynamics than those near other regions of the protein. Since this  $\beta$  turn is believed to play a critical role in the receptor binding of this protein, the faster dynamics of water near the  $\beta$  turn may have biological significance. The collective orientational dynamics of the water molecules in the protein solution exhibits a characteristic long time component of 27 ps, which agrees well with dielectric relaxation experiments.**

It is now generally accepted that the water molecules in the hydration shell around a protein play an important role in its biological activity, in addition to stabilizing the native state of the protein. Thus, an in-depth understanding of the dynamics of water molecules at the surfaces of proteins in aqueous solution is required to understand the functions of these biomolecules. This area has long been a subject of tremendous interest, being pursued by physicists, chemists and biologists alike<sup>1-4</sup>. Unfortunately, the dynamics of water molecules at heterogeneous surfaces are not easily amenable to direct experimental studies and as a result, progress has been rather slow, and the specific role of water in the activity of a given protein has often been left unclear.

In a series of recent papers, Vijayan and coworkers<sup>5,6</sup> have investigated the nature of hydration water by varying the humidity of hydrated proteins. They observed that the biological activity is lost at low humidity because the water molecules around the active sites are *more labile* than others in the hydration shell, and as a result, are the ones to be removed first. This is an interesting result

which suggests that in many cases the water molecules surrounding the active site can be more mobile so that they can participate in the ligand-binding process. This seems particularly true for lysozyme where the hydrophobic cavity is found to shrink in size due to water removal at high dehydration. It is, therefore, of great interest to understand the dynamics of water near the active sites. The questions that one would naturally ask, pertain to the reason for and the amplitude of the relative fastness of water near the active site. This knowledge can help us in developing a detailed understanding of protein's biological function. Vijayan and coworkers further found that in several proteins that they studied (lysozyme, ribonuclease and others), many of the water molecules in the hydration shell are used to stabilize the three-dimensional structure of the protein and these water molecules do so by forming bridges<sup>5,6</sup>. These water molecules are not easily removed upon dehydration. Thus, one may infer that the water molecules that stabilize the three-dimensional structure of proteins are dynamically slow while the ones that are biologically active are the relatively fast ones. Of course, such a generalization, however tempting, need not be universally valid, and requires a lot more work before any conclusion can be reached.

Among various experimental techniques that have been employed to understand the dynamics of water in the protein hydration shell, NMR, dielectric relaxation, and solvation dynamics in aqueous protein solutions have proved to be rather fruitful<sup>1,3,7-9</sup>. The discovery that water dynamics at the surfaces of biological macromolecules and of self-organized assemblies is much slower than what it is in bulk was first elucidated by dielectric relaxation (DR) experiments of aqueous protein solutions and colloids<sup>1,8,10,11</sup>. In all these systems, one typically finds an anomalous dispersion, in the range of 40–100 ps (called the  $\delta$  dispersion) which has been attributed to the water molecules at the surface of the macromolecule. As can be expected, these water molecules are much slower in their single particle dynamics than the water molecules in the bulk solution<sup>12-16</sup>. In addition to the study of DR, recently several solvation dynamics studies have been carried out on aqueous protein solutions, micelles (both normal and reverse), lipid vesicles and other similar systems using

\*For correspondence. (e-mail: bala@jncasr.ac.in; bbagchi@sscu.iisc.ernet.in)

the fluorescent probes located near the surface of the macromolecule/self-assembly<sup>7,18,17-21</sup>. In these solvation dynamics experiments too, a slow component has been observed. In some cases, this slow component was found to decay with a time constant in the range of 20–40 ps, which can be attributed to the dynamical exchange between free and bound water as mentioned above<sup>7</sup>.

In view of the discussions given above, one would expect that the water molecules in the hydration shell of protein should show a bimodal dynamics, to a first approximation. A part of the water molecules should continue to be mobile and fast (like their bulk counterpart) while a significant number should be slow. As remarked earlier, these 'free' and 'bound' water molecules could play quite different biological roles. This view seems to have been substantiated even in the case of the small protein we investigate here.

Several recent computer simulation studies have explored water dynamics near proteins, such as lysozyme which are moderate size proteins<sup>22-25</sup>. However, these studies are yet to explore the biological role of water in great detail. In this article, we present an atomistic molecular dynamics (MD) simulation of water molecules in a solution of a simple but biologically relevant protein. The protein that we study in this work is the toxic domain of heat stable enterotoxin (PDB ID: 1ETN). Heat stable enterotoxins (ST) are produced by *E. coli* bacteria in the intestine and are responsible for acute diarrhoea in humans and animals. They display a remarkable ability to retain their activity even at 100°C, hence the moniker, 'heat-stable'<sup>26</sup>. Similar enterotoxins are also secreted by other pathogenic bacteria. This class of peptides typically contain 18 or 19 amino acid residues, and share a common 13 amino acid sequence, which is<sup>27,28</sup>.

Cys<sup>5</sup>–Cys–Glu–Leu–Cys–Cys<sup>10</sup>–Asn–Pro–Ala–Cys–  
Ala<sup>15</sup>–Gly–Cys (Full peptide position)

Cys<sup>1</sup>–Cys–Glu–Leu–Cys<sup>5</sup>–Cys–Asn–Pro–Ala–Cys<sup>10</sup>–  
Ala–Gly–Cys (Toxic domain position)

Since this domain is conserved in several enterotoxins, one expects this 13 residue domain to be the primary reason for the toxicity of the 19-residue long protein. A striking feature of the toxic domain is the richness of sulphur containing cysteine residues. The six Cys residues form three disulphide bridges (between Cys<sup>5</sup> and Cys<sup>10</sup>; Cys<sup>6</sup> and Cys<sup>14</sup>; Cys<sup>9</sup> and Cys<sup>17</sup>), and provide stability to the ambient structure of the protein, and also probably aids in its heat stability<sup>29</sup>. In 1991, the group of Shimonishi<sup>30</sup> capped the first and the last Cys residues, and were able to crystallize this molecule. The residue '5' is the N-terminus and the residue '17' is the C-terminus. In the following, we refer to the residues with respect to their position in the full protein, in step with earlier workers<sup>28</sup>.

1ETN has a simple secondary structure: it has got 3 beta ( $\beta$ ) turns. The  $\beta_1$  spans from Cys<sup>6</sup> to Cys<sup>9</sup>,  $\beta_2$  from Asn<sup>11</sup> to Cys<sup>14</sup>, and  $\beta_3$  from Cys<sup>14</sup> to Cys<sup>17</sup>. In addition,

the crystal structure contains five intramolecular (i.e. within the protein) hydrogen bonds that also add to the stability of the conformation. The 1ETN structure is reasonably rigid (because of three disulphide bridges, and five intramolecular hydrogen bonds), making it an ideal candidate for studies by computer simulations using empirical intermolecular potentials.

Overall, this molecule has a hydrophobic character, as the side chains of all residues are oriented to the outside of the molecule. Specifically the side chains of Asn<sup>11</sup>, Pro<sup>12</sup>, and Ala<sup>13</sup> form a prominent, isolated cluster that projects from the surface to the outside of the molecule. As can be observed from Figure 1, where we display its structure obtained from X-ray crystallography, the interior of the protein is densely packed. Another interesting aspect of this protein is the presence of 13 water molecules in the crystal structure, which is rather large, considering the small size of the macromolecule. So, water is very important in stabilizing the beta turns. It is also known that specific residues in the first and the third beta turns can be replaced without losing the toxicity of the protein<sup>30</sup>. This implies that the second beta turn is most important for toxicity. Replacement of Ala<sup>13</sup> in the second turn decreases toxicity. It is also known that the residues near the second turn have hydrophobic side chains.

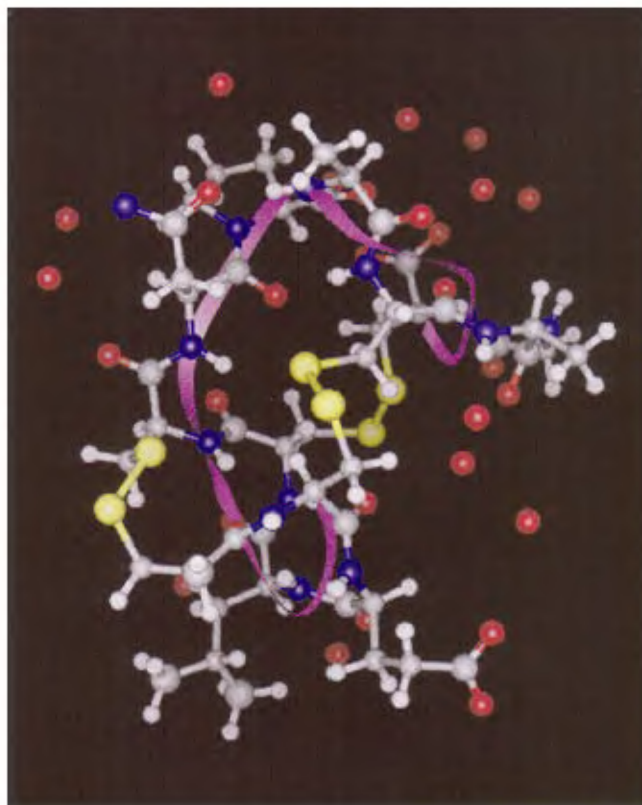


**Figure 1.** All-atom, ball and stick representation of the crystal structure of enterotoxin, 1ETN, along with the 13 'bound' water molecules that were observed with the crystal<sup>30</sup>.

In this first atomistic MD simulations on aqueous solution of 1ETN, we address the following specific issues: (1) How different is the structure of the protein in solution, obtained through our simulations from the reported crystal structure? (2) How different are the motions of water near the three segments of the protein? This question assumes additional importance in view of the supposed role of water molecules near Asn<sup>11</sup> residue in promoting binding to the enzyme<sup>31</sup>.

Our MD study of this solution reveals that water dynamics slows down *considerably* near the surface of the protein. Over and above this general slowdown, we observe a subtle difference in the reorientational dynamics of water molecules present near different segments of the protein. The total moment–moment time correlation function (measured in dielectric relaxation experiments) decays with a long time component of 27 ps.

## Simulation details

Atomistic molecular dynamics simulations of one molecule of 1ETN soaked in water were performed under constant volume and temperature conditions (NVT). The crystalline coordinates of the protein along with the ‘bound’ waters found in the crystal structure were taken as the initial configuration for the MD simulations. As mentioned earlier, Cys<sup>5</sup> is the N-terminus carrying a + 1.0e charge, and is capped with two hydrogen atoms, in our model. Cys<sup>17</sup> is the C-terminus with a – 1.0e charge, and is capped with an oxygen atom. In all, the capped protein contained 152 atoms. The three disulphide bonds were built into the model using rigid constraints. This configuration was then inserted into a well-equilibrated large box of water molecules, by carefully removing those water molecules which were within 2 Å from any atom of the protein molecule. The final system contained 2962 water molecules. Molecular dynamics calculations were performed using the PINY-MD computational program<sup>32</sup>. Temperature control was achieved using the Nosé-Hoover chains method, with a target temperature of 300 K. The simulations were carried out in a cubic box of edge length, 44.55 Å. The calculated average pressure of the system was about 22 atm, hence the system can be considered to be under ambient conditions. The reversible reference system propagator algorithm (RESPA) with an outer time step of 4 fs, was used to integrate the equations of motion. Initial MD runs were carried out with smaller timesteps to iron out further hard contacts between water molecules and the atoms of the protein. The CHARMM22 all-atom force fields<sup>33</sup> and potential parameters for proteins were employed to treat the interaction between atoms of the protein, while the TIP3P interaction model<sup>34</sup>, which is consistent with the CHARMM22 force fields, was used to describe the water molecules. Coulombic interactions were treated using the particle mesh Ewald method and

12,202 reciprocal space vectors were used in the lattice sum. The protein solution was equilibrated for about 2.5 ns, and the MD trajectory was extended further for analyses. In atomistic simulations of complex systems that exhibit varied time scales in their dynamics, it is difficult to store the configurations for analyses at high frequencies (say, every time step), as it requires vast amounts of storage. Hence, we have carried out MD runs (for analyses) of differing run lengths, which differ in the frequency with which configurations were stored. For instance, to obtain structural data, we used long runs (700 ps) with a time resolution of 1 ps, while for calculations of the ultra-fast component of the time correlation function (TCF) of water dipoles, we used relatively shorter trajectories of about 50 ps duration with a time resolution of 16 fs. The data presented in figure 5 was averaged over 11 such blocks, each of duration 50 ps. Successive blocks were separated by an interval of 25 ps to guarantee independent sampling. Thus the total length of the trajectory that was used for analyses is around 1.5 ns. We were thus able to meet the requirements, both of high accuracy and of reliability of these TCFs in the short timescales, as well as being able to probe the slow (long timescales) dynamics present in this complex system.

## Results and discussion

### *Protein structure and local dynamics*

In Figure 2, we show the secondary structure of the simulated protein in solution and compare it against that obtained from the crystalline sample. It should be noted that, unlike the structure in the crystalline state, the protein in solution is fluxional – this implies that at least a few configurations from the MD trajectory must be sampled and compared against the structure in the crystal. For this comparison, rigid body translations and rotations have been performed on the simulated structures to minimize the deviation from the crystal structure. In Figure 2, we show four such configurations. We find that the secondary structure of the simulated sample is essentially identical to the crystal structure, except for a marginal difference in the  $\beta_3$  segment of the protein. This is not unexpected, as the simulated protein is in solution, while the experimental structure corresponds to the crystal. Closer examinations indicate that the  $\beta_1$  and  $\beta_3$  segments are marginally closer to each other for the protein in solution than for the crystal.

As mentioned earlier, five intramolecular hydrogen bonds were observed in the experimental crystal structure. Only two of these five hydrogen bonds were found to be preserved during the entire MD trajectory, while the other three pair distances were found to be larger than the donor–acceptor bond lengths reported for the crystal. Thus, the solution structure is predicted to be different in

details from the crystal structure. The first of the two remaining H-bonds, the one between Cys<sup>14</sup> and Asn<sup>11</sup> was found to have a distance of  $3.16 \text{ \AA} \pm 0.01$  in the solution (simulation), compared with  $3.13 \text{ \AA}$  in the crystal (experiment). The second intramolecular hydrogen bond, between Ala<sup>13</sup> and Asn<sup>11</sup> was found to have a distance of  $3.16 \text{ \AA} \pm 0.02$  in simulation compared with  $2.89 \text{ \AA}$  in experiment.

It would be interesting to study the time dependence of the lengths of these two intramolecular hydrogen bonds. This will enable us to learn about the timescales involved in the correlated motion of the hydrogen bond. We have calculated the time autocorrelation function of the fluctuation in these bond lengths,  $C_{\text{ihb}}(t)$  as,

$$C_{\text{ihb}}(t) = \langle b(0)b(t) \rangle / \langle b \rangle, \quad (1)$$

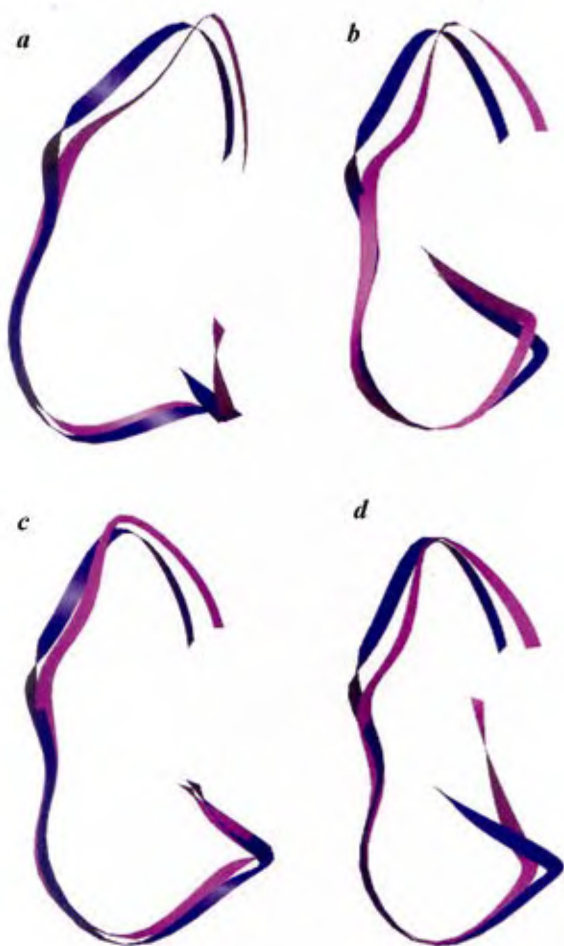


**Figure 2.** Secondary structure of representative configurations of the protein in solution obtained during the molecular dynamics trajectory, compared with the structure in the crystal. Blue: Configuration in the crystal; Magenta: Instantaneous configurations at different times of the MD trajectory, separated from the initial, crystalline configuration by *a*, 600 ps (1.96 Å); *b*, 1100 ps (2.43 Å); *c*, 2200 ps (2.02 Å); *d*, 2500 ps (2.51 Å). The root mean squared deviation between the coordinates of the crystalline and the MD configurations are shown in parentheses.

where  $b(t)$  is the bond length at a time  $t$ , and the angular brackets denote averaging over time origins,  $\{0\}$ . This function plotted in Figure 3, for the two intramolecular hydrogen bonds, exhibits interesting dynamics. The TCF for the hydrogen bond between Cys<sup>14</sup> and Asn<sup>11</sup> spanning the second  $\beta$  turn shows characteristic oscillations, with a period of about 250 fs signifying the breathing mode of the bond. However, we did not observe existence of such distinct breathing mode for the hydrogen bond between Ala<sup>13</sup> and Asn<sup>11</sup>. Another significant feature of the dynamics of these intramolecular bonds is the presence of a relatively slow time component in their decay. Although a large fraction of the TCF decays within about 500 fs, it is not until 3 ps that the correlation functions actually reach the zero value. These dynamical signatures could be expected to show up in the low frequency regime (less than  $100 \text{ cm}^{-1}$ ) in spectroscopic experiments. A similar dynamic study of the distance between the pairs that were H-bonded in the crystal but are more separated in solution should be interesting.

### Structure of water at the interface

As mentioned earlier, biochemical studies have shown the second  $\beta$  turn of enterotoxin to be proximal to the receptor. It is thus of interest to see if there are any significant differences between the structure of the water molecules around the three segments of the protein. We have calculated the simplest of a structural correlator – the pair correlation function between the interfacial water molecules and the protein. We display in Figure 4, the pair correlation function of water molecules with respect to the  $C_{\alpha}$  atom of the residues that form part of each of the three  $\beta$  turns. This provides us with an idea of the arrangement of water molecules in different sections around the protein, and the results are indeed interesting. The pair correlation function, for water molecules near the  $\beta_1$  and  $\beta_3$

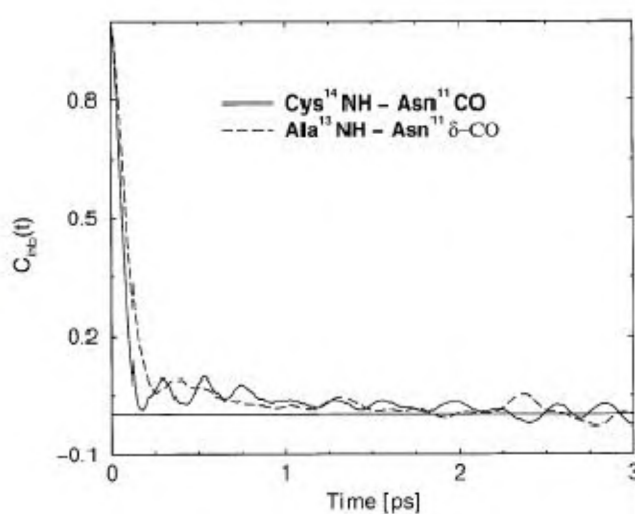


**Figure 3.** Auto-time correlation functions,  $C_{\text{ihb}}(t)$  of the donor-acceptor distance of two intramolecular hydrogen bonds of the protein.

segments exhibits a double-peaked feature, with one peak at around 4.0 Å, and another at around 4.75 Å. On the contrary, for water molecules near the  $\beta_2$  segment, the first hump at 4.0 Å is absent, while the peak at around 4.75 Å is observed.

It thus appears that the feature at 4.75 Å could be a general characteristic of water at the interface, while the feature at 4.0 Å might arise from specific interactions with residues in the first and the third  $\beta$  turn. These could probably be formation of hydrogen bonds between residues in these segments and water molecules favourably oriented towards them. We have examined water molecules that form pair distances with  $C_\alpha$  atoms between 3.6 Å and 4.1 Å, for  $C_\alpha$  atoms in each of these three turns, and have found that in *majority of cases, such water molecules form hydrogen bonds with the adjacent residues*. The absence of a clear peak in the  $g(r)$  corresponding to residues in the second  $\beta$  turn thus suggests a decrease in the number of water–protein hydrogen bonds in this segment, relative to that in  $\beta_1$  and  $\beta_3$  regions. This feature is likely to influence the dynamics of interfacial water molecules, as we note in the next section. We also note that the reduction in the intensity of the  $g(r)$  function implies a reduced first coordination number of water molecules for residues in the second  $\beta$  turn, as opposed to the other two turns.

#### Reorientational dynamics of water in hydration layer

Orientational response of water at the surface of proteins has been investigated both by dielectric relaxation and also by solvation dynamics experiments<sup>4</sup>. Of these two

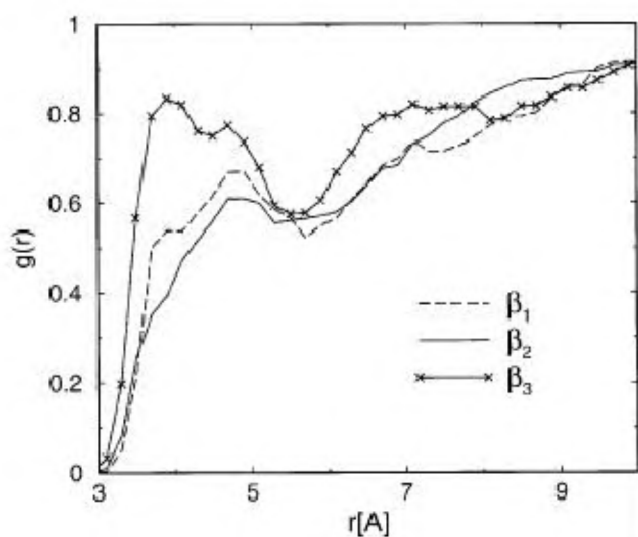


**Figure 4.** Pair correlation function,  $g(r)$ , of water molecules with respect to  $C_\alpha$  atom of the protein. The three curves correspond to the probability of finding a water molecule at a distance  $r$ , from any residue that is present in the first ( $\beta_1$ ), second ( $\beta_2$ ), and the third ( $\beta_3$ ),  $\beta$ -turn respectively.

techniques, it is the second one which partly probes single molecule orientation dynamics. Our earlier theoretical studies on the aqueous micellar solution have shown that single molecule orientational dynamics is a sensitive probe of surface forces<sup>12</sup>. We exploit this sensitivity to investigate the correlation between biological activity and water dynamics. We perform this in the following way. First, we tag all the water molecules within 5 Å of any atom of the side chains of the residues. We average the orientational correlation function over these water molecules only. The orientational correlation function is defined as

$$C_\mu(t) = \langle \vec{\mu}_i(0) \cdot \vec{\mu}_i(t) \rangle, \quad (2)$$

where  $\vec{\mu}_i(t)$  is the dipole vector of the water molecule  $i$ , and the angular brackets denote averaging over initial times as well as over water molecules that are present in the defined hydration layer. Second, we discriminate between these surface water molecules according to their proximity to different regions of the protein. This is based on the work of Shimonishi and coworkers who observed that the residues in the second  $\beta$  turn are proximal to the receptor in the binding of enterotoxin<sup>31</sup>. This ties in with the observation that the toxicity of the protein too is unaffected by changing specific residues in the first and the third  $\beta$  turns, while the activity was considerably affected when similar mutations were effected in the residues of the second  $\beta$  turn. In order to relate to these biochemical studies, we have classified the hydration layer of 1ETN into three regions, based on their proximity to each of the three  $\beta$  turns.

To summarize, we have calculated three distinct orientational correlation functions corresponding to the physical location of the water molecules relative to the protein. We now discuss the results. In Figure 5, we present  $C_\mu(t)$

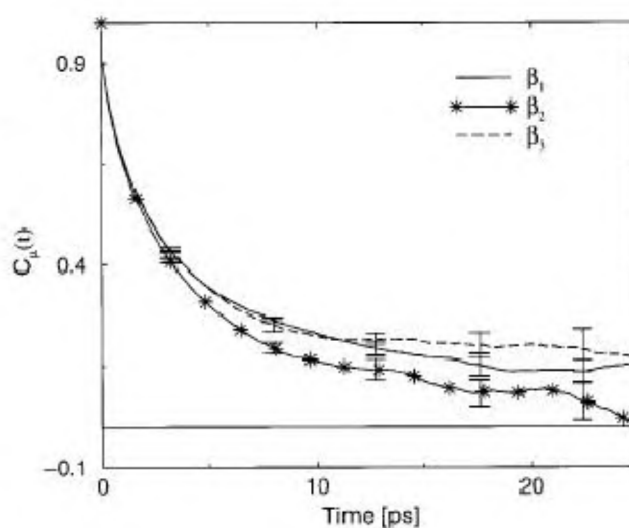


**Figure 5.** Reorientational time correlation function of the water dipole,  $C_\mu(t)$  for water molecules in the three segments of the protein. The vertical bars are error on the mean value of the TCF at specified times, and are displayed infrequently for clarity.



for the water molecules near the three segments of the protein. Water molecules near the  $\beta_2$  segment exhibit a considerably faster ability to reorient than those molecules near the first and the third segments of the protein. The active site of various proteins are, in general, hydrophobic in nature<sup>35,36</sup>. Our data shows that water molecules in the vicinity of the active site (the second segment of the enterotoxin molecule) exhibit faster dynamics in their ability to reorient their dipoles.

In order to quantify our observations, we have fitted the TCFs to a sum of three exponential functions. The parameters for best fit are shown in Table 1. The water molecules near the first and the third segment of the protein, exhibit significant slow dynamics with a long time component that unfortunately could not be quantified from our limited data. It is expected to be in the range of a few hundred picoseconds. This contribution could arise from water molecules that are hydrogen bonded to specific residues in these segments. Thus, the average time constant for reorientation of water dipoles in these segments is expected to be several times longer than the time constant found for water molecules near the second segment. A similar long time component with a time constant of around 14 ps is present for water molecules near the second segment of the protein. It should also be noted that the average time constant for dipolar reorientation of water molecules in any of these segments is much higher than that for an individual water molecule in bulk. The time constant for the latter is only 2.0 ps. Thus, although the reorientational dynamics of water is slowed down at the protein–water interface compared with pure water, noticeable differences in the dynamics arise, probably due to the interactions of specific, proximal residues, and to the local geometry of the protein.

### Collective moment time correlation function

Dielectric relaxation (DR) measures the collective polar response of a dipolar liquid. This is related to the total

dipole moment time correlation function of the system, which, at a given time  $t$ ,  $\vec{M}(t)$ , is defined as,

$$\vec{M}(t) = \sum_{i=1}^N \vec{\mu}_i(t), \quad (3)$$

where  $N$  is the total number of molecules and  $\vec{\mu}_i$  is the total dipole moment of the  $i$ th molecule. The complex dielectric function  $\epsilon(\omega)$  is given by the fluctuation–dissipation theorem<sup>37,38</sup>

$$\frac{\epsilon(\omega) - \epsilon(\infty)}{\epsilon(0) - \epsilon(\infty)} = \int_0^\infty dt \exp(-i\omega t) \left[ -\frac{d\phi(t)}{dt} \right] \\ = 1 - i\omega \int_0^\infty dt \exp(-i\omega t) \phi(t), \quad (4)$$

where  $\epsilon(\infty)$  and  $\epsilon(0)$  are the limiting low-frequency and high-frequency permittivities respectively.  $\phi(t)$  is the normalized time auto correlation function of the system's total dipole,  $\vec{M}$ , and is defined as

$$\phi(t) = \frac{\langle \vec{M}(t) \cdot \vec{M}(0) \rangle}{\langle \vec{M}(0) \cdot \vec{M}(0) \rangle}. \quad (5)$$

All the water molecules in the protein system have been considered to calculate the moment–moment time

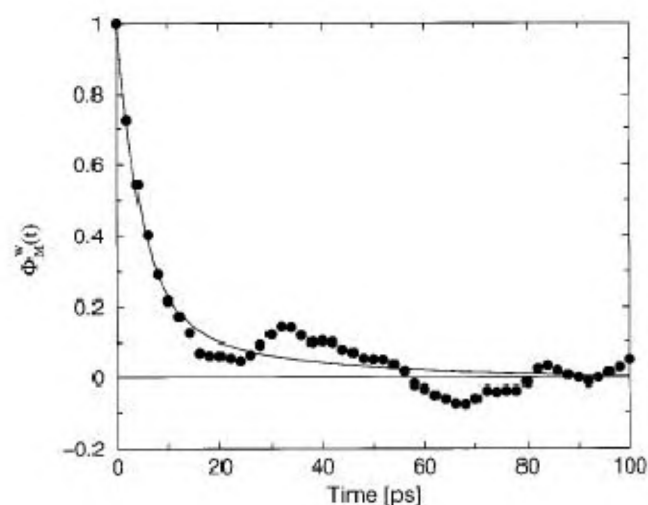


**Figure 6.** Time dependence of the normalized total moment–moment time correlation function for the water molecules ( $\Phi_M^w(t)$ ), in the protein solution. Circles are simulation data and the continuous line is the multiexponential fit.

**Table 1.** Parameters of multi-exponential fit to the dipole reorientational time correlation functions of water molecules near different segments of the protein, compared with that for water in bulk.  $\langle \tau_\mu \rangle$  is the average time constant. The time constant of the long time component for the  $\beta_1$  and  $\beta_3$  segments could not be ascertained due to limited data

Segment	Time constant (ps)	Amplitude (%)	$\langle \tau_\mu \rangle$ (ps)
$\beta_1, \beta_3$	0.32	22.4	–
	4.18	61.4	
	Large	16.2	
$\beta_2$	0.06	11.6	5.6
	1.97	48.2	
	11.44	40.2	
Bulk TIP3P water	0.27	20.2	2.0
	2.43	79.8	

**Table 2.** Parameters of multi-exponential fit to the moment–moment time correlation function of water molecules ( $\Phi_M^w(t)$ ), in the protein solution. The average time constant,  $\tau_M^w$ , for water molecules in the simulated protein solution and for bulk TIP3P water are shown for comparison

	Time constant (ps)	Amplitude (%)
$\langle \tau_M^w \rangle$ (ps)	4.8	81.8
	27.3	18.2
	8.9 (Protein)	7.3 (Bulk) (ref. 39)

correlation moment  $(\Phi_M^W)(t)$ , the contribution of water molecules alone to the total dielectric relaxation of the protein solution. Such an analysis helps us to identify components of the total relaxation that arise from interfacial and bulk states of water.

This TCF has been fitted into two exponentials, of the form

$$\Phi_M^W(t) = C_1 \exp(-t/\tau_1) + C_2 \exp(-t/\tau_2), \quad (6)$$

to get the time constants and amplitudes which are shown in Table 2. Note the appearance of a slow component of 27 ps in the total moment time correlation function. In the case of bulk (that is, neat) water, the decay is single exponential with a time constant of 7.3 ps. Our result of the appearance of a slow component is in agreement with experimental results. However, an understanding the origin of this slow component requires further study.

## Conclusions

We have presented here the study of a biologically relevant small protein, enterotoxin, in solution using atomistic molecular dynamics simulations. The calculations reveal that although the overall structure of the protein in solution is similar to that in its crystalline state, there are also significant differences – only two of the five hydrogen bonds survive in solution. In order to characterize the intramolecular vibrational degrees of freedom, we have probed the time correlation function of two intramolecular hydrogen bonds in the system. These show a low frequency dynamics with a time constant of around 250 fs, that can be probed through spectroscopy.

The significant role of water in mediating protein–receptor interactions has been well documented in the past. We observe a reduced structuring of water molecules near the second  $\beta$  turn of enterotoxin, as opposed to that near the first and the third  $\beta$  turns. Although the reorientational dynamics of water molecules in the hydration layer of the protein is slower than in pure water, the specifics of the dynamics is nuanced; we find *significantly*, the reorientation of water dipole to be faster for molecules near the second  $\beta$  segment than for those near the first and the third segments of the protein. It is worth noting that the earlier biochemical study of Shimonishi *et al.*<sup>31</sup>, implicated the second segment of enterotoxin to be the active region. The exact relationship of this work to our current results needs to be probed further. Within these simulations, it should also be possible to pinpoint the exact origin of the differential dynamics of water molecules across the three segments, and assign them to specific, water–residue interactions and probably to the dynamics of water–protein hydrogen bond<sup>41</sup>. Although we have shown this difference to arise from difference in pair correlation functions, this too needs to be studied further.

The collective dynamics of water that influences its ability to solvate other molecules, exhibits slow dynamics with a characteristic slow component of 27 ps. This is likely to come from water molecules in the hydration layer that are strongly bound to the biomolecule.

1. Grant, E. H., McClean, V. E. R., Nightingale, N. R. V., Sheppard, R. J. and Chapman, M. J., Dielectric behaviour of water in biological solutions—studies on myoglobin, human low-density-lipoprotein, and polyvinylpyrrolidone. *Bioelectromagnetics*, 1986, **7**, 151; Grant, E. H., South, G. P., Takashima, S. and Ichimura, H., Dielectric dispersion in aqueous solutions of oxyhaemoglobin and carboxy-haemoglobin. *Biochem. J.*, 1971, **122**, 691.
2. Pethig, R., Protein–water interactions determined by dielectric methods. *Annu. Rev. Phys. Chem.*, 1992, **43**, 177–205.
3. Denisov, V. P., Peters, J., Horlein, H. D., Halle, B., Using buried water molecules to explore the energy landscape of proteins. *Nature Struct. Biol.*, 1996, **3**, 505.
4. Nandi, N., Bhattacharyya, K. and Bagchi, B., Dielectric relaxation and solvation dynamics of water in complex chemical and biological systems. *Chem. Rev.*, 2000, **100**, 2013.
5. Nagendra, H. G., Sukumar, N. and Vijayan, M., Role of water in plasticity, stability, and action of proteins: The crystal structures of lysozyme at very low levels of hydration. *Proteins: Struct., Function Genet.*, 1998, **32**, 229–240.
6. Salunke, D. M., Veerapandian, B., Kodandapani, R. and Vijayan, M., Water-mediated transformations in protein crystals. *Acta Crystallogr., B*, 1985, **41**, 431–436; Salunke, D. M., Veerapandian, B. and Vijayan, M., Water-mediated structural transformations in a new crystal form of ribonuclease-A and tetragonal lysozyme. *Curr. Sci.*, 1984, **53**, 231–235.
7. Pal, S. K., Peon, J., Bagchi, B. and Zewail, A. H., Biological water: Femtosecond dynamics of macromolecular hydration. *J. Phys. Chem. B*, 2002, **106**, 12376.
8. Nandi, N. and Bagchi, B., Dielectric relaxation of biological water. *J. Phys. Chem. B*, 1997, **101**, 10954.
9. Mattos, C., Protein–water interactions in a dynamical world. *Trends Biochem. Sci.*, 2002, **27**, 203–208.
10. Gaiduk, V. I., In *Dielectric Relaxation and Dynamics of Polar Molecule*, World Scientific, Singapore, 1999.
11. Mashimo, S., Kuwabara, S., Yagihara, S. and Higasi, K., Dielectric relaxation time and structure of bound water in biological materials. *J. Phys. Chem.*, 1987, **91**, 6337; Fukuzaki, M. *et al.*, Comparison of water relaxation time in serum albumin solution using nuclear magnetic resonance and time domain reflectometry. *J. Phys. Chem.*, 1995, **99**, 431.
12. Balasubramanian, S. and Bagchi, B., Slow orientational dynamics of water molecules at a micellar surface. *J. Phys. Chem. B*, 2002, **106**, 3668–3672; Pal, S., Balasubramanian, S. and Bagchi, B., Identity, energy, and environment of interfacial water molecules in a micellar solution. *J. Phys. Chem. B*, 2003, **107**, 5194–5202.
13. Balasubramanian, S. and Bagchi, B., Slow solvation dynamics near an aqueous micellar surface. *J. Phys. Chem. B*, 2001, **105**, 12529–12533.
14. Balasubramanian, S., Pal, S. and Bagchi, B., Dynamics of water molecules at the surface of an aqueous micelle: Atomistic molecular dynamics simulation study of a complex system. *Curr. Sci.*, 2002, **82**, 845–854; Balasubramanian, S., Pal, S. and Bagchi, B., Evidence for bound and free water species in the hydration shell of an aqueous micelle. *Curr. Sci.*, 2003, **84**, 428–430.
15. Pal, S., Balasubramanian, S. and Bagchi, B., Temperature dependence of water dynamics at an aqueous micellar surface: Atomistic molecular dynamics simulation studies of a complex system. *J. Chem. Phys.*, 2002, **117**, 2852–2859.
16. Cheng, Y.-K. and Rossky, P. J., Surface topography dependence

- of biomolecular hydrophobic hydration. *Nature*, 1998, **392**, 696–699.
17. Vajda, S., Jimenez, R., Rosenthal, S. J., Fidler, V., Fleming, G. R. and Castner Jr., E., Femtosecond to nanosecond solvation dynamics in pure water and inside the  $\gamma$ -cyclodextrin cavity. *J. Chem. Soc. Faraday Trans.*, 1995, **91**, 867.
  18. Jordanides, X. J., Lang, M. J., Song, X. and Fleming, G. R., Solvation dynamics in protein environments studied by photon echo spectroscopy. *J. Phys. Chem. B*, 1999, **103**, 7995.
  19. Nandi, N. and Bagchi, B., Ultrafast solvation dynamics of an ion in the  $\gamma$ -cyclodextrin cavity: The role of restricted environment. *J. Phys. Chem.*, 1996, **100**, 13914–13919.
  20. Bhattacharyya, K., Solvation dynamics and proton transfer in supramolecular assemblies. *Acc. Chem. Res.*, 2003, **36**, 95.
  21. Pal, S. K., Peon, J. and Zewail, A. H., Biological water at the protein surface: Dynamical solvation probed directly with femtosecond resolution. *Proc. Natl. Acad. Sci. USA*, 2002, **99**, 1763–1768.
  22. Tarek, M. and Tobias, D. J., Environmental dependence of the dynamics of protein hydration water. *J. Am. Chem. Soc.*, 1999, 9740–9741; Tarek, M. and Tobias, D. J., The dynamics of protein hydration water: A quantitative comparison of molecular dynamics simulations and neutron-scattering experiments. *Biophys. J.*, 2000, **79**, 3244–3257.
  23. Bizzarri, A. R. and Cannistraro, S., Molecular dynamics of water at the protein–solvent interface. *J. Phys. Chem. B.*, 2002, **106**, 6617–6633.
  24. Marchi, M., Sterpone, F. and Ceccarelli, M., Water rotational relaxation and diffusion in hydrated lysozyme. *J. Am. Chem. Soc.*, 2002, **124**, 6787–6791.
  25. Xu, H. and Berne, B. J., Hydrogen-bond kinetics in the solvation shell of a polypeptide. *J. Phys. Chem. B*, 2001, **105**, 11929–11932.
  26. Smith, H. W. and Gyles, C. L., The relationship between two apparently different enterotoxins produced by enteropathogenic strains of *Escherichia coli* of porcine origin. *J. Med. Microbiol.*, 1970, **3**, 387–401.
  27. Gariepy, J. *et al.*, Structure of the toxic domain of *Escherichia coli* heat-stable enterotoxin ST I. *Biochemistry*, 1986, **25**, 7854–7866.
  28. Sato, T., Ozaki, H., Hata, Y., Kitagawa, Y., Katsube, Y. and Shimonishi, Y., Structural characteristics for biological activity of heat-stable enterotoxin produced by enterotoxigenic *Escherichia coli*: X-ray crystallography of weakly toxic and nontoxic analogs. *Biochemistry*, 1994, **33**, 8641–8650.
  29. Shimonishi, Y. *et al.*, Mode of disulfide bond formation of a heat-stable enterotoxin (STh) produced by a human strain of enterotoxigenic *Escherichia coli*. *FEBS Lett.*, 1987, **215**, 165–170.
  30. Ozaki, H., Sato, T., Kubota, H., Hata, Y., Katsube, Y. and Shimonishi, Y., Molecular structure of the toxin domain of heat-stable enterotoxin produced by a pathogenic strain of *Escherichia coli*: A putative binding site for a binding protein on rat intestinal epithelial cell membranes. *J. Biol. Chem.*, 1991, **266**, 5934.
  31. Hasegawa, M., Kawano, Y., Matsumoto, K., Hidaka, Y., Sato, T. and Shimonishi, Y., Identification of a binding region on *Escherichia coli* heat-stable enterotoxin to intestinal guanylyl cyclase C. *Lett. Pept. Sci.*, 1997 **4** 1–11.
  32. Tuckerman, M. E., Yarne, D. A., Samuelson, S. O., Hughes, A. L. and Martyna, G. J., Exploiting multiple levels of parallelism in molecular dynamics based calculations via modern techniques and software paradigms on distributed memory computers. *Comp. Phys. Commun.*, 2000, **128**, 333.
  33. Mackerell Jr. A. D. *et al.*, All-atom empirical potential for molecular modeling and dynamics studies of proteins. *J. Phys. Chem. B*, 1998, **102**, 3586.
  34. Jorgensen, W. L., Chandrasekhar, J., Madura, J. D., Impey, R. W. and Klein, M. L., Comparison of simple potential functions for simulating liquid water. *J. Chem. Phys.*, 1983, **79**, 926.
  35. Ringe, D., What makes a binding site a binding site? *Curr. Opin. Struct. Biol.*, 1995, **5**, 825–829.
  36. Janin, J., Wet and dry interfaces: The role of solvent in protein–protein and protein–DNA recognition. *Structure*, 1999, **7**, R277–R279.
  37. Williams, G., Use of the dipole correlation function in dielectric relaxation. *Chem. Rev.*, 1972, **72**, 55.
  38. Zwanzig, R., Time-correlation functions and transport coefficients in statistical mechanics. *Annu. Rev. Phys. Chem.*, 1965, **61**, 67.
  39. Höchtel, P., Boresch, S., Bitomsky, W. and Steinhauser, O., Rationalization of the dielectric properties of common three-site water models in terms of their force field parameters. *J. Chem. Phys.*, 1998, **109**, 4927.
  40. Huang, C. C., Couch, G. S., Pettersen, E. F. and Ferrin, T. E., Pacific Symposium on Biocomputing, 1996, vol. 1, pp. 724. (<http://www.cgl.ucsf.edu/chimera/>).
  41. Balasubramanian, S., Pal, S. and Bagchi, B., Hydrogen bond dynamics near a micellar surface: Origin of the universal slow relaxation at complex aqueous interfaces. *Phys. Rev. Lett.*, 2002, **89**, 115505-1-115505-4.

**ACKNOWLEDGEMENTS.** We thank Prof. Hemalatha Balam and Prof. M. Vijayan for many helpful discussions. This study was supported in part by grants from the Department of Biotechnology (DBT), the Council of Scientific and Industrial Research (CSIR) and the Department of Science and Technology (DST), New Delhi. Government of India. The visualizations in Figure 1 and 3 were produced using the Chimera package from the Computer Graphics Laboratory, University of California, San Francisco<sup>40</sup>.

Received 12 September 2003; revised accepted 5 November 2003